THE JOURNAL OF BIOLOGICAL CHEMISTRY VOL. 281, NO. 46, pp. 35327–35335, November 17, 2006
Printed in the U.S.A.

Helix 8 of the Viral Chemokine Receptor ORF74 Directs Chemokine Binding*

Received for publication, July 19, 2006, and in revised form, September 20, 2006 Published, JBC Papers in Press, September 22, 2006, DOI 10.1074/jbc.M606877200

Dennis Verzijl[‡], Leonardo Pardo[§], Marie van Dijk[‡], Yvonne K. Gruijthuijsen[¶], Aldo Jongejan[‡], Henk Timmerman[‡], John Nicholas[‖1], Mario Schwarz[**], Philip M. Murphy[**], Rob Leurs[‡], and Martine J. Smit[‡2]

*From the [‡]Leiden/Amsterdam Center for Drug Research, Division of Medicinal Chemistry, Vrije Universiteit Amsterdam, De Boelelaan 1083, 1081 HV Amsterdam, The Netherlands, the [§]Laboratorio de Medicina Computacional, Unidad de Bioestadistica, Facultad de Medicina, Universidad Autonoma de Barcelona, 08193 Barcelona, Spain, the [¶]Department of Medical Microbiology, Cardiovascular Research Institute Maastricht, University of Maastricht, P. O. Box 5800, 6202 AZ Maastricht, The Netherlands, the [‖]Molecular Virology Laboratories, Sidney Kimmel Comprehensive Cancer Center, The Johns Hopkins University, Baltimore, Maryland 21231, and the **Laboratory of Molecular Immunology, NIAID, National Institutes of Health, Bethesda, Maryland 20892*

The constitutively active G-protein-coupled receptor and viral oncogene ORF74, encoded by Kaposi sarcoma-associated herpesvirus (human herpesvirus 8), binds a broad range of chemokines, including CXCL1 (agonist), CXCL8 (neutral ligand), and CXCL10 (inverse agonist). Although chemokines interact with the extracellular N terminus and loops of the receptor, we demonstrate that helix 8 (Hx8) in the intracellular carboxyl tail (C-tail) of ORF74 directs chemokine binding. Partial deletion of the C-tail resulted in a phenotype with reduced constitutive activity but intact regulation by ligands. Complete deletion of the C-tail, including Hx8, resulted in an inactive phenotype that lacks CXCL8 binding sites and has an increased number of binding sites for CXCL10. Similar effects were obtained with the single R7.61^{322}W or Q7.62^{323}P mutations in Hx8. We propose that the conserved charged or polar side chain at position 7.61 has a specific role in stabilizing the end of transmembrane domain 7 (TM7). Disruption of Hx8 by deletion or mutation distorts an H-bonding network, involving highly conserved amino acids within TM2, TM7, and Hx8, that is crucial for positioning of the TM domains, coupling to Gαq, and CXCL8 binding. Thus, Hx8 appears to exert a key role in receptor stabilization through the conserved residue R7.61, directing the ligand binding profile of ORF74 and likely also that of other class A G-protein-coupled receptors.

Viral G-protein-coupled receptors (GPCRs)[3] have attracted considerable attention over the past few years. Although for most viral GPCRs, their role in viral pathogenesis still has to be elucidated, for the Kaposi sarcoma-associated herpesvirus-encoded receptor ORF74, a clear link to Kaposi sarcoma has been established (1). Due to their homology with human chemokine receptors and the acquisition of additional properties, such as constitutive activity and promiscuous G-protein coupling and chemokine binding, viral GPCRs provide unique insight in the molecular mechanisms of chemokine receptor function. ORF74 shares homology with the CXC chemokine receptor family and with CXCR2 in particular (see Ref. 2 for an overview of chemokine receptors and nomenclature). In general, human chemokine receptors bind only a subset of chemokines. Interestingly, ORF74 binds a broad range of chemokines with unique pharmacology. Several CXCR2 ligands act as agonist (*e.g.* CXCL1/GROα (growth-related oncogene α)), partial agonist, neutral ligand (*e.g.* CXCL8/IL-8 (interleukin-8)), or inverse agonist. Both CXCR3 and CXCR4 ligands, CXCL10/IP-10 (γ-interferon-inducible protein-10) and CXCL12/SDF-1α (stromal cell-derived factor 1-α), respectively, act as inverse agonists (3). Previously, it was demonstrated that both CXCL1 and CXCL10 bind with high affinity either to a common conformation of ORF74 or to readily interconvertible states, not available for the neutral ligand CXCL8 (3). Also, for other class A GPCRs known to bind more than one ligand, *e.g.* the tachykinin NK1 receptor (4) and chemokine receptors CXCR2 (5), CXCR3 (6), and US28 (7), binding modes appear clearly distinct for the different ligands. This phenomenon is associated with the inability of some of these ligands to displace each other and/or a clear difference in the apparent number of binding sites (B_{max}), suggesting that these ligands bind to distinct receptor populations (8). For chemokine receptors, the binding mode is defined by interaction of chemokines with the extracellular N terminus and loops of their cognate receptors (9, 10) as well as by the activation state of the receptor (6).

In this study, we demonstrate that also the intracellular side of the receptor, more particularly Hx8 in the C-tail of ORF74, directs chemokine binding. Mutational analysis and receptor modeling studies show that disruption of the intracellular Hx8 distorts the H-binding network crucial for positioning of the transmembrane domains and interaction with Gα_q, thereby inducing differential chemokine binding to ORF74. Thus, posi-

* This work was supported in part by grants from The Netherlands Organization for Scientific Research (NWO Jonge Chemici grant) (to D. V. and R. L.), the Royal Netherlands Academy of Arts and Sciences (KNAW) (to M. J. S.), and the European Community (Grant LSHB-CT-2003-503337) and Ministerio de Educacion y Ciencia (Grant SAF2006-04966) (to L. P.) The costs of publication of this article were defrayed in part by the payment of page charges. This article must therefore be hereby marked "*advertisement*" in accordance with 18 U.S.C. Section 1734 solely to indicate this fact.
[1] Supported by National Institutes of Health Grants CA76445, CA119887, and CA113239.
[2] To whom correspondence should be addressed. Tel.: 31-20-5987572; Fax: 31-20-5987610; E-mail: MJ.Smit@few.vu.nl.
[3] The abbreviations used are: GPCR, G-protein coupled receptor; C-tail, carboxyl tail; EGFP, enhanced green fluorescent protein; HA, influenza hemagglutinin epitope; Hx8, helix 8; IP-10, γ-interferon-inducible protein-10; NF-κB, nuclear factor-κ B; ORF74, open reading frame 74; PLC, phospholipase C; TM, transmembrane domain; WT, wild type; ELISA, enzyme-linked immunosorbent assay.

tioning of Hx8 of ORF74 appears to be a key determinant in directing chemokine binding.

EXPERIMENTAL PROCEDURES

Materials—Cell culture media, penicillin, and streptomycin were obtained from Invitrogen, and fetal bovine serum was purchased from Integro B.V. (Dieren, The Netherlands). *myo*-[2-^{3}H]Inositol (17 Ci/mmol) and ^{125}I-labeled CXCL1, CXCL8, and CXCL10 (2,200 Ci/mmol) were obtained from PerkinElmer Life Sciences. Chemokines were obtained from PeproTech (Rocky Hill, NJ).

DNA Constructs—The cDNA of the HHV-8-encoded ORF74 (GenBank^{TM} accession number U71368 with a silent G → T mutation at position 927) was a gift from T. Schwartz and inserted in pcDEF$_3$ (a gift from J. A. Langer (11)) after PCR amplification. ORF74 C-tail deletion mutants were constructed using PCR. Constructs were tagged at the N terminus with the influenza virus hemagglutinin (HA) epitope using PCR or subcloning. pEGFP-N1 constructs containing cDNA encoding ORF74-WT, Δ12, and Δ24 have been described before (12). pSG5-ORF74-R^{322}W and -Q^{323}P were previously described (13). The NF-κB reporter plasmid pNF-κB-Luc was obtained from Stratagene (La Jolla, CA).

Cell Culture and Transfection—COS-7 cells were grown at 5% CO_2 at 37 °C in Dulbecco's modified Eagle's medium supplemented with 5% fetal bovine serum, penicillin (50 IU/ml), and streptomycin (50 μg/ml). COS-7 cells were transiently transfected with 2 μg of ORF74 construct or empty vector (mock transfection) per million cells using DEAE-dextran.

ELISA—COS-7 cells were transfected with cDNA encoding HA-tagged ORF74 constructs or empty vector (mock transfection). Forty-eight hours after transfection, cells were washed with Tris-buffered saline and fixed with 4% paraformaldehyde in phosphate-buffered saline. After blocking with 1% skim milk in 0.1 M $NaHCO_3$ (pH 8.6), cells were incubated with mouse monoclonal anti-HA antibody (a gift from J. van Minnen) in Tris-buffered saline containing 0.1% bovine serum albumin, washed three times with Tris-buffered saline, and incubated with goat anti-mouse horseradish peroxidase-conjugated secondary antibody (Bio-Rad). Subsequently, cells were incubated with substrate buffer containing 2 mM *o*-phenylenediamine (Sigma), 35 mM citric acid, 66 mM Na_2HPO_4, 0.015% H_2O_2 (pH 5.6). The reaction was stopped with 1 M H_2SO_4, and absorption at 490 nm was determined.

Confocal Imaging—Transfected COS-7 cells were grown on glass coverslips. After 48 h, confocal images were collected at a wavelength of 488 nm and processed as described previously (14).

Phospholipase C Activation—Twenty-four h after transfection, COS-7 cells were labeled overnight in Earle's inositol-free minimal essential medium supplemented with *myo*-[2-^{3}H]-inositol (2 μCi/ml). Cells were washed with Dulbecco's modified Eagle's medium containing 20 mM LiCl and 25 mM HEPES (pH 7.4) and incubated for 2 h in the same medium in the presence or absence of indicated chemokines (100 nM). Inositol phosphates were isolated as described previously (15) and counted by liquid scintillation.

NF-κB Reporter Gene Assay—COS-7 cells were co-transfected with pNF-κB-Luc (5 μg/10^6 cells) and indicated ORF74 constructs (2 μg/10^6 cells). Transfected cells were seeded in 96-well white plates (Costar) in serum-free culture medium and incubated with the indicated chemokines (100 nM) for 48 h, after which NF-κB-driven luciferase expression was measured by aspiration of the medium and the addition of 25 μl of luciferase assay reagent (0.83 mM ATP, 0.83 mM D-luciferin, 18.7 mM $MgCl_2$, 0.78 μM $Na_2H_2P_2O_7$, 38.9 mM Tris (pH 7.8), 0.39% (v/v) glycerol, 0.03% (v/v) Triton X-100, and 2.6 μM dithiothreitol). Luminescence was measured for 3 s in a Wallac Victor^2.

Binding Experiments—Transfected COS-7 cells were seeded in 48-well plates. After 48 h, binding was performed on whole cells for 4 h at 4 °C using ^{125}I-labeled chemokines (~100 pM) in binding buffer (50 mM HEPES (pH 7.4), 1 mM $CaCl_2$, 5 mM $MgCl_2$, 0.5% bovine serum albumin) in the presence or absence of unlabeled chemokine. After incubation, cells were washed three times with ice-cold binding buffer supplemented with 0.5 M NaCl. Subsequently, cells were lysed and counted in a Wallac Compugamma counter. Total protein per well was determined with lysed cells using the BCA protein assay (Pierce).

Construction of the ORF74 Receptor Model—A model of the ORF74 receptor was constructed by homology modeling using the crystal structure of rhodopsin (Protein Data Bank code 1U19) (16) as template. The following amino acids were aligned: N^{55}-N1.50^{65} (the superscripts represent the residue numbering in the rhodopsin structure and ORF74 sequence, respectively, and 1.50 is the standardized numbering for GPCRs according to Ballesteros and Weinstein (17), based on the most conserved amino acid in each TM helix). The first number refers to the helix in which the amino acid is located, and the second number indicates the position relative to the most conserved amino acid at position 50 in that helix, *i.e.* N1.50, D2.50, R3.50, W4.50, P5.50, P6.50, and P7.50), N^{73}-D2.40^{83}, R^{135}-R3.50^{143}, P^{215}-P5.50^{223}, P^{267}-P6.50^{266}, and P^{303}-P7.50^{311}. The absence of W4.50 in the ORF74 receptor makes the orientation of TM4 arbitrary. The amino acids at the intracellular C-terminal domain are numbered relative to P^{303}-P7.50^{311}. Thus, the highly conserved Phe side chain in Hx8 is F^{313}-F7.60^{321}. A detailed description of the procedure to obtain the molecular models of wild type and mutant receptors has been reported elsewhere (18).

RESULTS

Deletion of C-tail Does Not Affect ORF74 Expression—ORF74-WT and C-tail deletion mutants of ORF74 (Δ12 and Δ24 amino acids) were constructed (Fig. 1*A*). The constructs were also tagged at the N terminus with the HA epitope or C-terminally fused with enhanced green fluorescent protein (EGFP) (12). All constructs were expressed at the cell surface to a similar degree as wild type (WT) ORF74 in COS-7 cells, as assessed by ELISA with a monoclonal anti-HA antibody (Fig. 1*B*). Confocal microscopic images of cells expressing ORF74-WT-EGFP, Δ12-EGFP, and Δ24-EGFP confirmed that these receptors show similar expression patterns (Fig. 1*C*).

Gα$_q$-mediated Signaling Is Modulated by Deletion of the C-tail of ORF74—ORF74 activates phospholipase C (PLC) in the absence of ligands through activation of Gα$_q$ proteins (19–

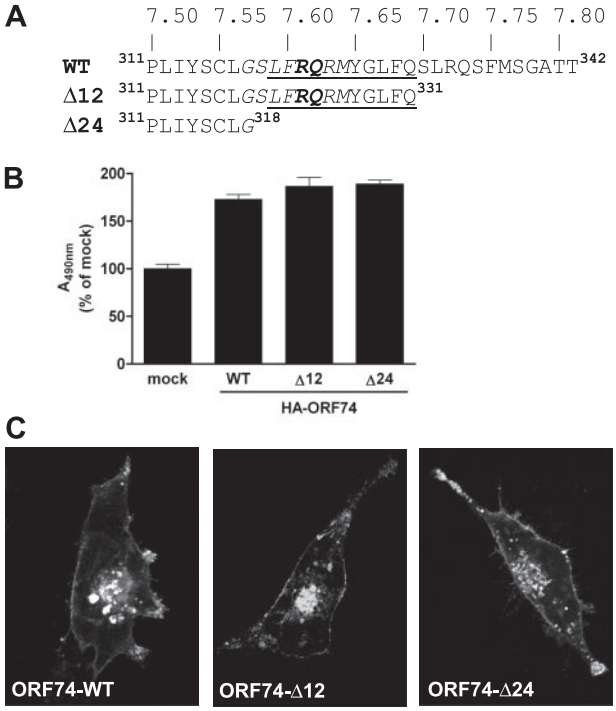

FIGURE 1. **Expression of ORF74 deletion mutants.** *A*, schematic representation of the C-tail of ORF74-WT and mutants. Residues downstream of the conserved Pro at the end of TM7 (P7.50^{311}) are shown. R7.61^{322} and Q7.62^{323} are shown in *bold*. The region conserved among γ-herpesvirus GPCRs is depicted in *italics*, and Hx8 is *underlined*. *B*, ELISA with HA-tagged. COS-7 cells were transfected with cDNA encoding N-terminally HA-tagged ORF74 constructs or empty vector. Forty-eight hours after transfection, expression of the HA-tagged receptors was determined using an anti-HA antibody in an ELISA. Data are presented as the percentage of the absorption displayed by mock-transfected (*mock*) cells. A representative experiment performed in triplicate is shown. The experiment was repeated three times. *C*, confocal microscopy with EGFP-tagged ORF74. Representative pictures of COS-7 cells were made after transfection with C-terminally EGFP-tagged ORF74 constructs.

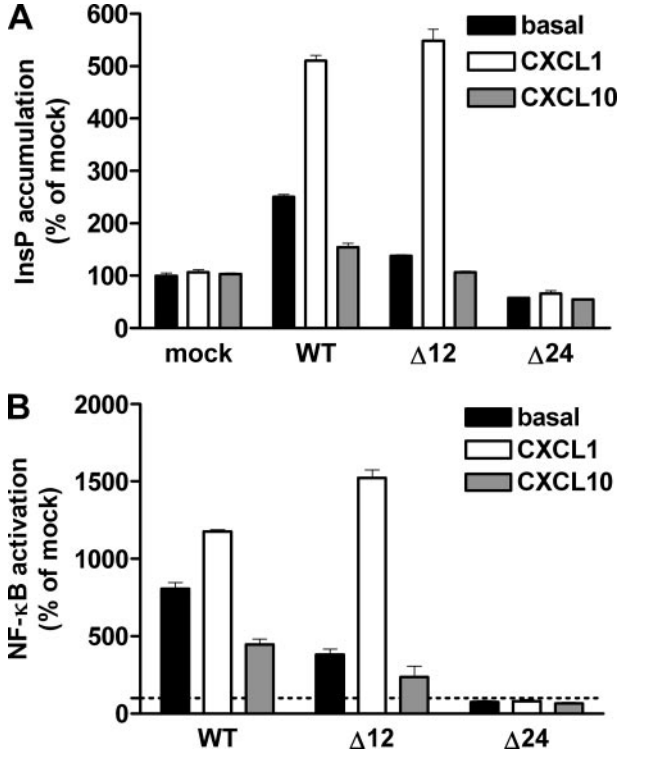

FIGURE 2. **Signal transduction of ORF74 deletion mutants.** *A*, activation of PLC. COS-7 cells were transfected with HA-tagged ORF74 constructs or empty vector. After 48 h, inositol phosphates accumulation was determined for 2 h in the absence (*black bars*) or presence of 100 nM CXCL1 (*white bars*) or CXCL10 (*gray bars*). *mock*, mock-transfected. *B*, activation of NF-κB. COS-7 cells were cotransfected with pNF-κB-Luc and HA-tagged ORF74 constructs or empty vector and incubated in the presence or absence of chemokines (100 nM). NF-κB-mediated luciferase expression was determined after 48 h. Data are presented as the percentage of unstimulated mock-transfected cells. Representative experiments performed in triplicate are shown. The experiments were repeated three times.

21). ORF74-Δ12 was less efficient than WT in constitutive activation of PLC, whereas ORF74-Δ24 lacked all constitutive activity (Fig. 2*A*). The level of activation of ORF74-Δ12 by the agonist CXCL1 was comparable with WT. In contrast, ORF74-Δ24 did not respond to CXCL1. The inverse agonist CXCL10 inhibited basal signaling of ORF74-WT and Δ12, whereas Δ24 was unaffected by incubation with CXCL10 as expected since ORF74-Δ24 did not display constitutive activity. Similar results were obtained when ORF74-mediated NF-κB activation was measured using a NF-κB-luciferase reporter gene (Fig. 2*B*). These data indicate that the C-tail of ORF74 is important for $G\alpha_q$-mediated signal transduction.

C-tail Directs Chemokine Binding Profile of ORF74—The observed reduction in constitutive signaling could be a consequence of the expression of improperly folded receptors, which cannot be discriminated from functional receptors by the ELISA and confocal microscopy experiments shown in Fig. 1. Therefore, binding experiments with the radiolabeled neutral ligand CXCL8 were performed. ^{125}I-CXCL8 binding to ORF74-Δ12 was reduced when compared with WT (Fig. 3*A*). Moreover, ORF74-Δ24 did not bind ^{125}I-CXCL8 at all. Similar experiments were performed with the radiolabeled inverse agonist CXCL10. Surprisingly, a gradual increase in ^{125}I-CXCL10 binding was observed upon deletion of C-terminal amino acids when compared with WT (Fig. 3*A*). ORF74-Δ24, which did not bind ^{125}I-CXCL8, showed the most pronounced increase in ^{125}I-CXCL10 binding.

Binding with the radiolabeled agonist CXCL1 was unaffected for ORF74-Δ12 or Δ24 (Fig. 3*B*). Furthermore, the affinity of all tested chemokines for the deletion mutants did not change significantly when compared with ORF74-WT, as determined with homologous displacement curves (Fig. 3, *C–E*). Interestingly, different numbers of binding sites were obtained for the radiolabeled chemokines. For CXCL8, the observed B_{max} varied between ~300 (WT) and 0 (Δ24) fmol/mg of protein. The B_{max} values for CXCL1 and CXCL10 were about 10-fold higher in the 1–5 pmol/mg of protein range. Notably, B_{max} values for CXCL1 were consistently higher than for CXCL10. Therefore, it appears that the C-tail of ORF74 influences the chemokine binding profile of ORF74.

Chemokine Binding Profile of ORF74 Correlates with Proper $G\alpha_q$ Interaction—We previously showed that several residues of the C-tail distal to the seventh transmembrane domain affect functional G-protein coupling (13). In particular, the ORF74-R^{322}W mutant (R7.61^{322}W, according to the standardized GPCR numbering (17), see "Experimental Procedures") was unable to couple functionally to $G\alpha_q$ in the absence of ligands in HEK293 cells. Another mutant, ORF74-Q^{323}P (Q7.62^{323}P), was

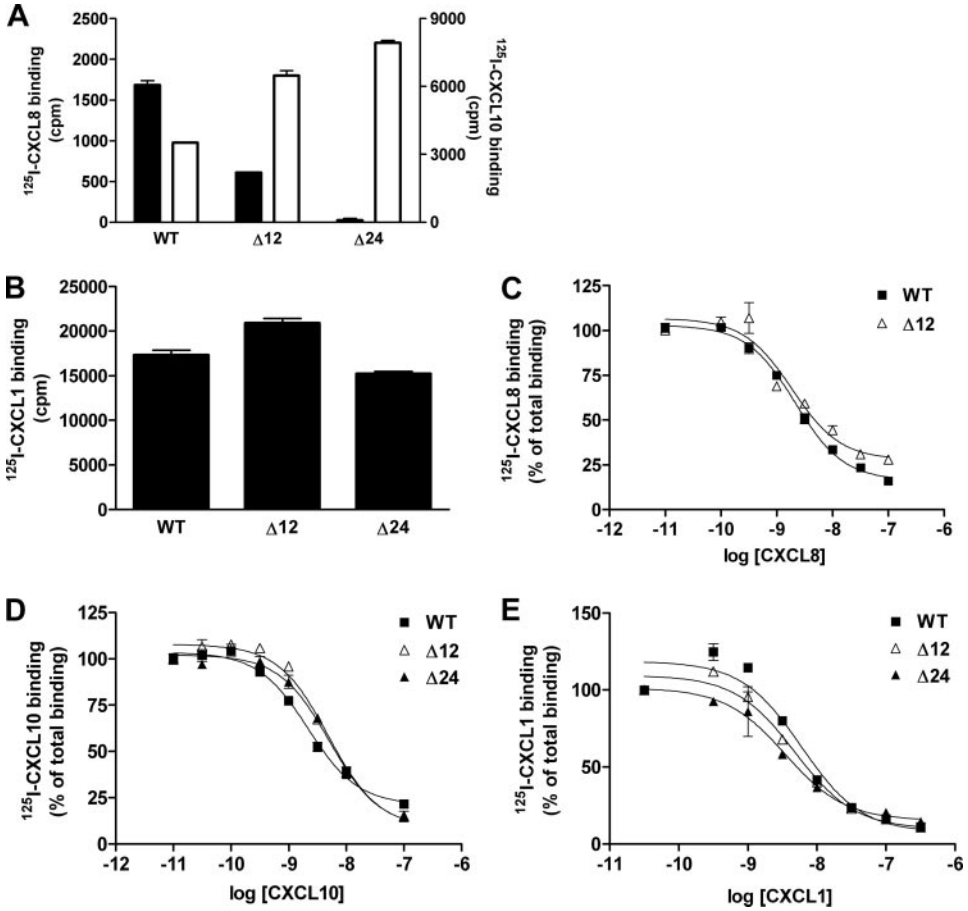

FIGURE 3. **Chemokine binding profile of ORF74 deletion mutants.** COS-7 cells were transfected with the indicated HA-tagged ORF74 constructs. *A*, binding experiments with ^{125}I-labeled CXCL8 (*black bars*, *left axis*) and CXCL10 (*white bars*, *right axis*) were performed in the absence (total binding) or presence (unspecific binding) of unlabeled homologous chemokine (100 nM). *B*, binding experiments with ^{125}I-CXCL1 were performed in the absence (total binding) or presence (unspecific binding) of unlabeled CXCL1 (100 nM). Data are presented as specific binding (total binding − unspecific binding) in cpm. *C–E*, homologous displacement curves were generated in the presence of increasing concentrations of unlabeled chemokine. Data are presented as the percentage of total binding of each construct. For CXCL8, pIC_{50} values (the negative log of the concentration of cold ligand at which the amount of bound radioligand is reduced with 50%) were 8.6 and 8.8 for ORF74-WT and Δ12, respectively. The pIC_{50} value for Δ24 could not be determined since this mutant did not bind ^{125}I-CXCL8. pIC_{50} values for CXCL10 were 8.5, 8.5, and 8.4 for WT, Δ12, and Δ24, respectively. For CXCL1, the pIC_{50} values were 7.9, 8.1, and 8.1, respectively, for WT, Δ12 and Δ24. Representative experiments performed in triplicate are shown. The experiments were repeated at least two times.

unable to constitutively activate both $G\alpha_q$- and $G\alpha_i$-mediated signaling pathways in HEK293 cells (13) (Fig. 1*A*). In this study, we further analyzed the effect of these mutations on signaling and chemokine binding properties. Both ORF74-R^{322}W and -Q^{323}P mutants were unable to constitutively activate PLC in COS-7 cells (Fig. 4*A*), consistent with their inability to constitutively activate $G\alpha_q$. However, ORF74-R^{322}W activated PLC-mediated signaling when incubated with the agonist CXCL1, whereas ORF74-Q^{323}P did not activate PLC in the presence of CXCL1. The inverse agonist CXCL10 inhibited constitutive signaling of WT, and signaling of the constitutively inactive mutants was unaffected by CXCL10 as expected. Next, we investigated activation of NF-κB by both point mutants. ORF74-R^{322}W and ORF74-Q^{323}P did not constitutively activate NF-κB in COS-7 cells (Fig. 4*B*). However, both mutants could be stimulated with CXCL1 in this assay, although activation of NF-κB by ORF74-Q^{323}P was only marginal. As expected, no effect on signaling of the inactive mutants was observed for the inverse agonist CXCL10 (Fig. 4*B*). Subsequently, binding experiments with radiolabeled CXCL8, CXCL10, and CXCL1 were performed. Similar to ORF74-Δ12, ORF74-R^{322}W displayed a reduced number of CXCL8 binding sites, whereas the number of CXCL10 binding sites was increased when compared with WT (Fig. 5*A*). As seen for ORF74-Δ24, ORF74-Q^{323}P did not bind CXCL8 at all, although it showed more binding sites for CXCL10 when compared with WT (Fig. 5*A*). All receptors had a comparable number of binding sites for CXCL1 (Fig. 5*B*). The observed changes in the amount of CXCL8 and CXCL10 binding could not be explained by a change in affinity of the ligands for the mutants (Fig. 5, *C–E*) but was a result of a change in the number of binding sites. Summarizing, the ability of the C-tail of ORF74 to functionally interact with $G\alpha_q$ correlates with its chemokine binding profile.

ORF74 C-tail Directs the Number of Binding Sites Accessible to Each Individual Ligand—Both CXCL1 and CXCL10 bind with high affinity to a common conformation of the receptor or to readily interconvertible states, not available for CXCL8 (3). We therefore determined whether the change in the number of binding sites for CXCL8 and CXCL10 could be explained by a change in the number of receptor states that are accessible for these ligands. To this end, heterologous displacement experiments were performed with the mutants that showed the most extreme differences in chemokine binding when compared with ORF74-WT, *i.e.* Δ24 and Q^{323}P. Interestingly, although CXCL8 and CXCL10 could not effectively displace ^{125}I-CXCL1 from ORF74-WT, CXCL10 could displace part of the bound ^{125}I-CXCL1 from the constitutively inactive mutants ORF74-Δ24 and -Q^{323}P (Fig. 6*A*). All chemokines could effectively displace ^{125}I-CXCL8 from ORF74-WT (Fig. 6*B*). Heterologous displacement of ^{125}I-CXCL8 from the ORF74-Δ24 and -Q^{323}P mutants could not be performed since they do not bind CXCL8. CXCL8 could not effectively displace ^{125}I-CXCL10 from ORF74-WT, -Δ24, or -Q^{323}P (Fig. 6*C*). In contrast, CXCL1 could displace ^{125}I-CXCL10 effectively from all mutants (Fig. 6*C*), even from ORF74-Δ24 and -Q^{323}P, which showed an increase in total ^{125}I-CXCL10 binding (Figs. 3*A* and 5*A*, respectively). Summarizing, the binding sites of ^{125}I-CXCL1 and ^{125}I-CXCL10 are not available for CXCL8. Furthermore, the num-

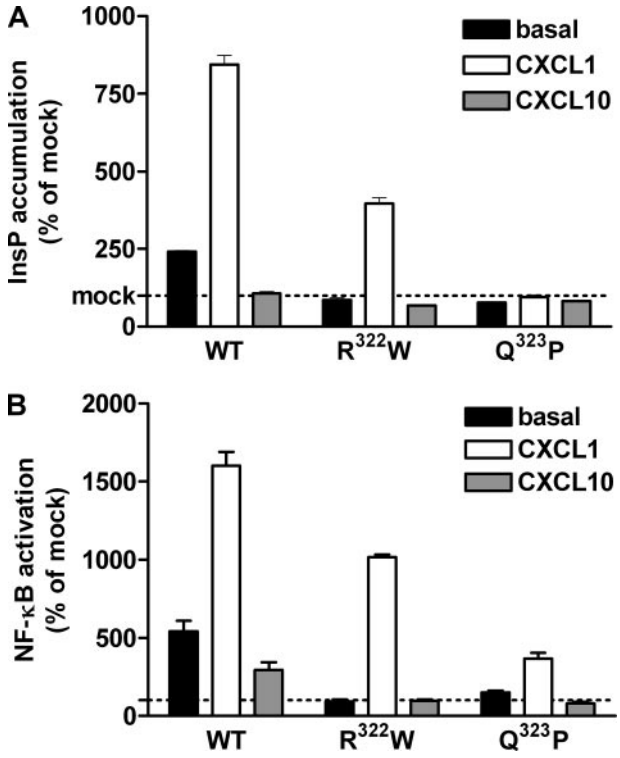

FIGURE 4. **Signal transduction of ORF74-$R^{322}W$ and -$Q^{323}P$.** *A*, activation of PLC. COS-7 cells were transfected with ORF74 constructs or empty vector. After 48 h, inositol phosphates accumulation was determined for 2 h in the absence (*black bars*) or presence of 100 nM CXCL1 (*white bars*) or CXCL10 (*gray bars*). *mock*, mock-transfected. *B*, activation of NF-κB. COS-7 cells were cotransfected with pNF-κB-Luc and ORF74 constructs or empty vector and incubated in the presence or absence of chemokines (100 nM). NF-κB-mediated luciferase expression was determined after 48 h. Data are presented as the percentage of unstimulated mock-transfected cells. Representative experiments performed in triplicate are shown. The experiments were repeated three times.

ber of ^{125}I-CXCL1 binding sites that are accessible for CXCL10 differs between ORF74-WT and both mutants, indicating a shift in receptor states for the mutants.

ORF74 Model Predicts a Key Role for Hx8 in Receptor Stabilization—To explain the observed changes in chemokine binding properties upon alteration of the C-tail, a receptor model based on the crystal structure of rhodopsin (16) was constructed. The membrane-proximal residues of the C-tail are part of the predicted Hx8 of ORF74 (Fig. 1*A*, *underlined*). Fig. 7, *A* and *B*, show TM7 (*blue*, up to C7.55^{316}), Hx8 that expands parallel to the membrane (*dark red*, from L7.59^{320} to Q7.69^{330}), and the following C-tail that changes direction to cover Hx8 (S7.70^{331}-T7.81^{342}). The ORF74-Δ12 mutant lacks the C-tail up to Hx8, whereas ORF74-Δ24 does no longer possess Hx8 (Fig. 7, *A* and *B*).

The stability of α-helices is achieved by the hydrogen bond between the carbonyl oxygen of residue i to the N–H amide atoms of residue i+4 in the following turn of the helix. Notably, the backbone carbonyl oxygens of residues at positions S7.54^{315} and C7.55^{316} do not possess their backbone N–H counterparts because they are located at the bottom of TM7 (Fig. 7*B*). Instead, the polar head group of R7.61^{322} stabilizes these free, helix-ending carbonyls through hydrogen bond interactions (Fig. 7*B*). The transition from TM7, perpendicular to the membrane, to Hx8, parallel to the membrane, is accomplished through the non-helical amino acids at positions L7.56^{317}-S7.58^{319}. S7.58^{319} contains the first backbone carbonyl engaged in the intramolecular hydrogen bond network that stabilizes Hx8 (Fig. 7*A*). The electronic nature of the carbonyl oxygen allows the formation of a hydrogen bond with both the N–H group of the residue in the following turn of the helix and the side chain of Q7.62^{323} in ORF74 (Fig. 7*A*). When Q7.62^{323} is mutated to Pro (ORF74-Q^{323}P), this interaction cannot take place (Fig. 7*C*).

Fig. 7*D* shows the interaction of Y7.53^{314} in TM7 with F7.60^{321} in Hx8 and with D2.40^{83} in TM2. The residues Y7.53 and F7.60 are highly conserved in the rhodopsin family of GCPRs (92 and 68%, respectively) and form the NP$XXYX_{5,6}$F motif (22). The Asp (D2.40^{83}) at the intracellular boundary of TM2 is conserved among chemokine receptors and has previously been shown to affect signaling of ORF74 (23). The hydroxyl group of Y7.53^{314} forms hydrogen bonds with the O_δ group and the carbonyl oxygen (via a water molecule) D2.40^{83} in TM2 (Fig. 7*D*).

DISCUSSION

The recent x-ray structure of rhodopsin, the prototype of class A receptors, revealed the presence of a highly conserved amphipathic eight helix (24). Based on this x-ray structure, it has been predicted that Hx8 interacts with the N-terminal helix of Gα and Gβγ subunits (25), implying its involvement in G-protein coupling. Although for some GPCRs, Hx8 appears dispensable for signaling (26), the importance of Hx8 in G-protein interaction has been shown, *e.g.* for the oxytocin receptor (27), bradykinin receptors (28), the angiotensin II receptor type 1A (29), the leukotriene B4 receptor (30), and the β_1-adrenergic receptor (31). Moreover, the N-terminal portion of Hx8 of the protease-activated receptor PAR1 was found to be involved in coupling to $G\alpha_q$, through a network of H-bond and ionic interactions, connecting Hx8 to the conserved NP$XXYX_{5,6}$F motif on TM7 and also to the adjacent intracellular loop 1 (32).

In this study, we show that Hx8 of ORF74 is an important determinant for constitutive activity, and more importantly, chemokine binding, using functional, binding, and computational approaches. Deletion of up to 12 amino acids of the C-tail resulted in reduced constitutive activation of PLC and NF-κB but not of agonist activation by CXCL1 (Fig. 2). Deletion of the entire C-tail including Hx8, however, resulted in a completely inactive receptor. The gradual loss of constitutive activity of ORF74-Δ12 and Δ24 was accompanied by a striking reduction in binding sites for CXCL8 and an increase in binding sites for CXCL10 (Fig. 3*A*). We therefore hypothesized that impaired coupling to $G\alpha_q$ caused the change in the chemokine binding pattern of ORF74. To test this hypothesis, we used ORF74-mutants (R^{322}W and Q^{323}P) in a region of the C-tail that is conserved in γ-herpesvirus-encoded GPCRs (Fig. 1*A*). Some of the amino acids in this region are also conserved in cellular chemokine receptors (13). We have previously shown in HEK293 cells that both mutants were unable to constitutively activate $G\alpha_q$-mediated signaling pathways and that R^{322}W could not couple functionally to $G\alpha_q$, although R^{322}W and $G\alpha_q$ were still able to physically interact (13). Also in COS-7 cells,

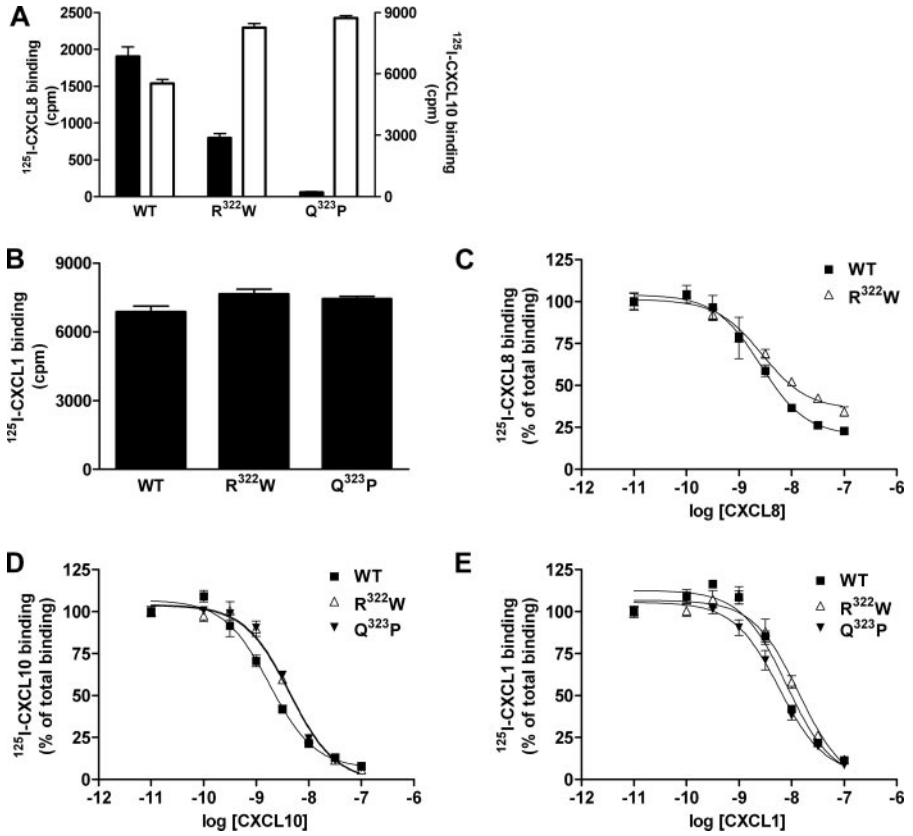

FIGURE 5. **Chemokine binding profile of ORF74-R^{322}W and -Q^{323}P.** COS-7 cells were transfected with indicated ORF74 constructs. *A*, binding experiments with ^{125}I-labeled CXCL8 (*black bars*) and CXCL10 (*white bars*) were performed in the absence (total binding) or presence (unspecific binding) of unlabeled homologous chemokine (100 nM). *B*, binding experiments with ^{125}I-CXCL1 were performed in the absence (total binding) or presence (unspecific binding) of unlabeled CXCL1 (100 nM). Data are presented as specific binding (total binding − unspecific binding) in cpm. *C–E*, homologous displacement curves were generated in the presence of increasing concentrations of unlabeled chemokine. Data are presented as the percentage of total binding of each construct. The pIC$_{50}$ values for CXCL8 were 8.6 and 8.5 for ORF74-WT and -R^{322}W, respectively. The pIC$_{50}$ value for Q^{323}P could not be determined since this mutant did not bind ^{125}I-CXCL8. For CXCL10, the pIC$_{50}$ values were 8.6, 8.3, and 8.4 for ORF74-WT, -R^{322}W, and -Q^{323}P, respectively. For CXCL1, the pIC$_{50}$ values were 8.3, 8.0, and 8.2, respectively, for WT, R^{322}W, and Q^{323}P. Representative experiments performed in triplicate are shown. The experiments were repeated at least two times.

ORF74-R^{322}W and -Q^{323}P did not constitutively activate Gα_q-mediated signal transduction pathways (Fig. 4). However, when stimulated with CXCL1, ORF74-R^{322}W activated PLC and NF-κB, indicating that ligand-induced Gα_q activation for R^{322}W is still intact. In contrast, ORF74-Q^{323}P could not activate PLC upon stimulation with CXCL1 (Fig. 4*A*), and CXCL1 only marginally stimulated NF-κB through ORF74-Q^{323}P (Fig. 4*B*), demonstrating that ORF74-Q^{323}P is deficient in activating Gα_q. The marginal activation of NF-κB upon CXCL1 stimulation of ORF74-Q^{323}P might be ascribed to the high sensitivity of the NF-κB assay or due to coupling to other G-proteins as Gα_{12}/Gα_{13} that have been shown to be involved in ORF74-mediated signaling (33). ORF74-R^{322}W showed reduced CXCL8 binding, whereas Q^{323}P was devoid of CXCL8 binding. Thus, the mutants that showed a reduction but not a complete loss of CXCL8 binding have reduced (Δ12) or no (R^{322}W) constitutive Gα_q-mediated signaling, but both have intact ligand-induced Gα_q-mediated signaling (Figs. 2 and 4). The mutants that showed a complete loss of CXCL8 binding (Δ24 and Q^{323}P) show no Gα_q-mediated signaling at all (Figs. 2 and 4). Therefore, we explain the drop in CXCL8 binding as a result of a decreased (Δ12 and R^{322}W) or impaired (Δ24 and Q^{323}P) ability to functionally interact with Gα_q.

Based on these findings, we suggest that the neutral ligand CXCL8 only binds to a constitutively active receptor conformation that has to be able to functionally couple to Gα_q proteins (R*Gα_q) (Fig. 8). The increase in the number of CXCL10-binding sites of the mutants is due to a shift from active (R*Gα_q) to inactive (R) receptor conformations. Being an inverse agonist, CXCL10 is predicted to preferably bind to inactive receptor conformations (34). This hypothesis is confirmed by the data in Fig. 6*A* where CXCL10 displaces ^{125}I-CXCL1 from the inactive mutants Δ24 and Q^{323}P but not from WT. The inability of CXCL10 to efficiently displace ^{125}I-CXCL1 from ORF74-WT (Fig. 6*A*) indicates an intermediate receptor state (R*) that is accessible to CXCL1 but not to CXCL10 (Fig. 8). Alternatively, CXCL1 and CXCL10 may bind in an allotopic manner to the same receptor state, as was suggested for the binding of CXCL10 and CXCL11 to CXCR3 (6). The number of binding sites of the agonist CXCL1 for all mutants is comparable with WT, suggesting that CXCL1 binds to all receptor conformations and that loss of binding to active receptor conformations is compensated by binding to inactive conformations. ORF74-Δ12 displays some constitutive activity and CXCL8 binding, although Hx8 is still present in this mutant. However, it can be envisioned that deletion of the last 12 amino acids already destabilizes Hx8 and its interactions with Gα_q, resulting in a phenotype that mostly exists in the R and R* states, and to a lesser extent, in the CXCL8 binding R*Gα_q state. ORF74-Q^{323}P or ORF74-Δ24 do not functionally interact with Gα_q at all and are predicted to be mainly in the inactive R state that does not bind CXCL8.

We have previously reported that ORF74-Δ5 fused to EGFP is unable to activate NF-κB and AP-1 in HEK293 cells (12). Moreover, NIH-3T3 cells expressing ORF74-Δ5-EGFP lacked surface-independent growth in soft agar, in contrast to ORF74-WT-EGFP, although ORF74-Δ5-EGFP still induced secretion of vascular endothelial growth factor comparable with ORF74-WT in these cells (12). However, both ORF74-Δ5 (data not shown) and the shorter variant ORF74-Δ12 (Fig. 2) are still capable of constitutively activating NF-κB and PLC in COS-7 cells. This indicates that ORF74-Δ5-EGFP might be defective in certain signaling pathways in HEK293 and NIH-3T3 cells,

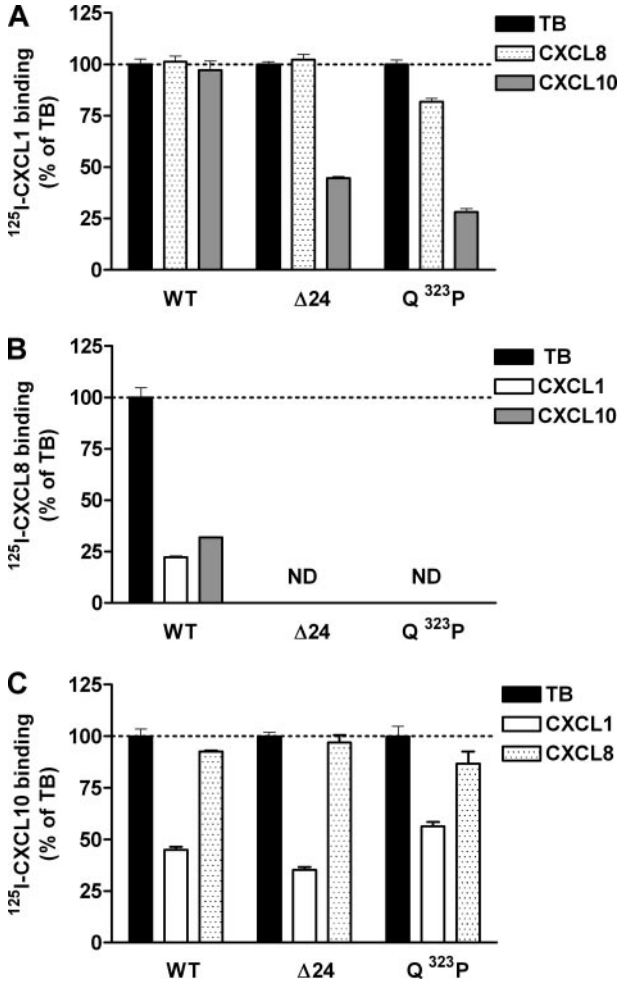

FIGURE 6. **Heterologous chemokine displacement.** COS-7 cells were transfected with indicated ORF74 constructs. After 48 h, heterologous displacement experiments were performed with radiolabeled CXCL1 (*A*), CXCL8 (*B*), or CXCL10 (*C*) in the absence (*black bars*, total binding) or presence of 100 nM cold CXCL1 (*white bars*), cold CXCL8 (*spotted bars*), or cold CXCL10 (*gray bars*). *ND*, not determined since ORF74-Δ24 and -Q^{323}P do not bind ^{125}I-CXCL8. Representative experiments performed in triplicate are shown. The experiments were repeated at least two times.

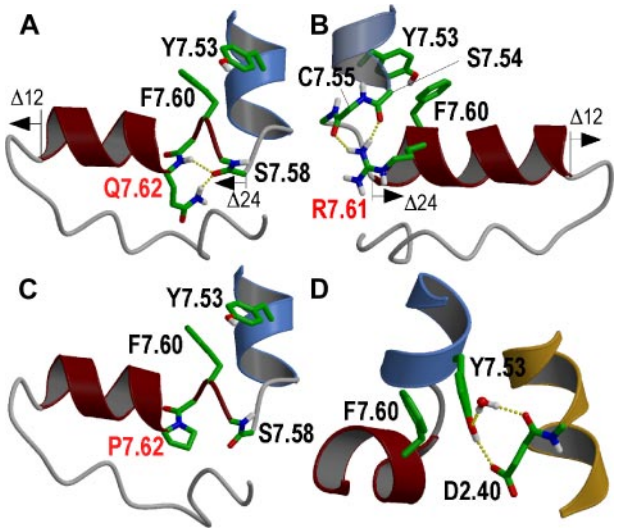

FIGURE 7. **The microenvironment of TM7.** Shown are TM7 (*blue*, up to C7.55^{316}), Hx8 that expands parallel to the membrane (*dark red*, from L7.59^{320} to Q7.69^{330}), and the following C-terminal tail that changes the direction to cover Hx8 (S7.70^{331}-T7.81^{342}). The positions in which ORF74-Δ12 and Δ24 were truncated are shown. *A*, a detailed view of the hydrogen bond interactions between the carbonyl oxygen of S7.58^{319} at the beginning of Hx8 and Q7.62^{323} through both its backbone N–H amide and polar side chain. *B*, the interaction of the polar head group of R7.61^{322} with the free, helix-ending carbonyl groups of residues S7.54^{315} and C7.55^{316} located at the end of TM7. *C*, replacement of Q7.62^{323} by Pro in the Q7.62^{323}P mutation removes both the polar side chain and the backbone N–H group, preventing the formation of any type of intramolecular hydrogen bond interaction. *D*, the interactions of Y7.53^{314} in TM7 with D2.40^{83} in TM2 (*goldenrod*) and F7.60^{321} in Hx8.

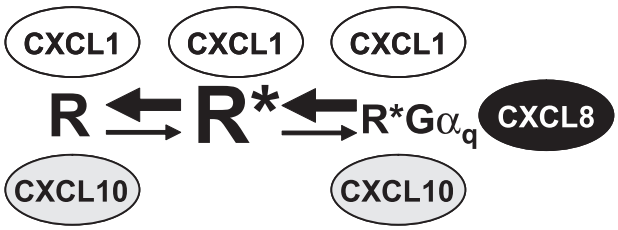

FIGURE 8. **Model for chemokine binding to ORF74 receptor states.** The uncoupled inactive receptor state R, the active state R*, and the active receptor state coupled to $G\alpha_q$, R*$G\alpha_q$, are shown. Possible interactions with other G-proteins are not shown for simplicity. The number of receptors in state R is larger than the number of receptors in state R*$G\alpha_q$. CXCL1 binds to all receptor states, whereas CXCL10 displaces CXCL1 only from R and R*$G\alpha_q$ and CXCL8 only binds to R*$G\alpha_q$. Upon gradual deletion of the C-tail as well as for ORF74-R^{322}W and -Q^{323}P, a shift takes place in favor of the inactive R conformation (*bold arrow*), resulting in a loss of R* and R*$G\alpha_q$ conformations. Therefore, the number of CXCL8 binding sites decreases, and the number of binding sites recognized by CXCL10 increases. The number of binding sites for CXCL1, which has affinity for all states, remains constant.

either due to their distinct cellular context or due to the presence of a C-terminal EGFP tag.

Fig. 7*D* shows the interaction of Y7.53^{314} in TM7 with F7.60^{321} in Hx8. These residues are part of the highly conserved NP*XXYX*$_{5,6}$F motif (22). It has been suggested that this aromatic-aromatic interaction is disrupted during receptor activation, leading to a proper realigning of Hx8 (22, 35). We suggest, on the basis of our observations and previous work by others (32, 36), that additional interactions between TM7 and Hx8 are necessary to maintain these helices at the proper orientation for constitutive activity and chemokine binding. The R7.61^{322} side chain of ORF74 interacts with the carbonyl groups of residues S7.54^{315} and C7.55^{316} located at the end of TM7 (Fig. 7*B*). We speculate that the absence of this interaction in the R7.61^{322}W mutant within Hx8 modifies TM7 and the binding site for chemokines at the extracellular part of the receptor. Position 7.61 is conserved in the rhodopsin-like family of GPCRs, holding a positively charged residue in 71% of the sequences (Lys, 17%; Arg, 54%) and a polar Gln side chain in other 11% of the sequences (37). All these polar side chains can form hydrogen bond interactions with both backbone carbonyls. We propose that the conserved side chain at position 7.61 has a specific role both in stabilizing the end of TM7 and in aligning Hx8 relative to the helical bundle of TM7 in the rhodopsin-like family of GPCRs.

The intramolecular hydrogen bond between the backbone carbonyl oxygen of residue S7.58^{319} at the beginning of Hx8 and Q7.62^{323} through both its backbone N–H amide and its side chain (Fig. 7*A*) seems another important element in defining the conformation of Hx8 relative to the helical bundle. Position 7.62 is partially conserved in the rhodopsin family of GPCRs since it contains a positively charged residue in 46% of the

sequences (Lys, 20%; Arg, 26%) and a polar side chain in other 24% of the sequences (Ser, 5%; Thr, 2%; Asn, 7%; Gln, 7%; His, 3%) (37). Notably, the Q7.62^{323}P mutation introduces a Pro-kink (38) in Hx8, removing both the polar side chain and the backbone N–H hydrogen bond interaction with the backbone carbonyl oxygen of residue S7.58^{319} (Fig. 7*C*). Most likely, the Q7.62^{323}P mutation modifies the conformation of R7.61^{322} and its interaction with the carbonyl groups at the end of TM7 (Fig. 7*B*), and of F7.60^{321} and its interaction with Y7.53^{314} in TM7 (Fig. 7*C*). In addition, the hydroxyl group of Y7.53^{314} forms hydrogen bonds with the O_δ group and the carbonyl oxygen (via a water molecule) of the partly conserved D2.40^{83} in TM2 (Asn, 40%; Asp, 10%), which has been proposed to play an important role in ORF74 signaling (23). Interestingly, D2.40 is conserved among most chemokine receptors, indicating a possible common intramolecular network. Variation of these key intracellular interactions between TM7, TM2, and Hx8 modifies the binding site for chemokines at the extracellular part of the receptor. The ORF74-Δ24 truncation completely removes Hx8, resulting in an inactive receptor that does not bind CXCL8.

Taken together, our results not only imply the importance of Hx8 for Gα_q coupling but show that positioning of Hx8 directs the chemokine binding profile of ORF74. Although a causative link between the loss of Gα_q-mediated signaling and loss of CXCL8 binding as proposed in Fig. 8 appears apparent, one might not rule out the occurrence of separate phenomena. Disruption of the interaction of TM7 with Hx8 might interfere with both CXCL8 binding and Gα_q coupling.

Our results clearly demonstrate that CXCL1, CXCL10, and CXCL8 bind to distinct ORF74 receptor populations (Figs. 6 and 8), explaining the apparent differences in B_{max}. Similar to findings for CXCR3 (6), the CXCL8-accesible, G-protein coupled state of ORF74 forms only a fraction of the total amount of receptor. The peptide ligands of GPCRs such as CXCR2, CXCR3, US28, and the NK1 receptor all show non-competitive behavior and differences in B_{max} in binding studies (4–7). Sequence conservation implies that most class A GPCRs have an intracellular Hx8 (25). The importance of Hx8, and in particular the H-bonding network involving the conserved residue R7.61, in directing receptor-ligand interactions might therefore be extrapolated to other class A GPCRs.

Additionally, G-proteins and adapter proteins (25, 39–42) have been reported to bind to Hx8 or to the NP*XXYX*$_{(5,6)}$F motif (43). Binding of these proteins to Hx8 or phosphorylation of residues within Hx8 might influence its integrity and H-bonding properties and thereby affect receptor-ligand interactions. ORF74-mediated tumorgenesis is not only dependent on constitutive activity of the receptor but also on regulation by endogenously expressed chemokines (44). Since ORF74 couples to a variety of G-proteins, the G-protein expression profile of infected cells might influence the relative amount of ORF74 in active and inactive conformations, thereby affecting the ability of individual chemokines to bind and signal efficiently. As such, Hx8 and proteins binding to Hx8 appear crucial determinants that direct not only signaling but also ligand binding. Thus, the cellular context and phosphorylation state of chemokine receptors might control chemokine binding properties and limit the known apparent chemokine redundancy (2) in general.

REFERENCES

1. Jensen, K. K., Manfra, D. J., Grisotto, M. G., Martin, A. P., Vassileva, G., Kelley, K., Schwartz, T. W., and Lira, S. A. (2005) *J. Immunol.* **174,** 3686–3694
2. Murphy, P. M., Baggiolini, M., Charo, I. F., Hebert, C. A., Horuk, R., Matsushima, K., Miller, L. H., Oppenheim, J. J., and Power, C. A. (2000) *Pharmacol. Rev.* **52,** 145–176
3. Rosenkilde, M. M., and Schwartz, T. W. (2000) *Mol. Pharmacol.* **57,** 602–609
4. Holst, B., Hastrup, H., Raffetseder, U., Martini, L., and Schwartz, T. W. (2001) *J. Biol. Chem.* **276,** 19793–19799
5. Ahuja, S. K., Lee, J. C., and Murphy, P. M. (1996) *J. Biol. Chem.* **271,** 225–232
6. Cox, M. A., Jenh, C.-H., Gonsiorek, W., Fine, J., Narula, S. K., Zavodny, P. J., and Hipkin, R. W. (2001) *Mol. Pharmacol.* **59,** 707–715
7. Kledal, T. N., Rosenkilde, M. M., and Schwartz, T. W. (1998) *FEBS Lett.* **441,** 209–214
8. Kenakin, T. (2001) *FASEB J.* **15,** 598–611
9. Leong, S. R., Kabakoff, R. C., and Hebert, C. A. (1994) *J. Biol. Chem.* **269,** 19343–19348
10. Ho, H. H., Du, D., and Gershengorn, M. C. (1999) *J. Biol. Chem.* **274,** 31327–31332
11. Goldman, L. A., Cutrone, E. C., Kotenko, S. V., Krause, C. D., and Langer, J. A. (1996) *BioTechniques.* **21,** 1013–1015
12. Schwarz, M., and Murphy, P. M. (2001) *J. Immunol.* **167,** 505–513
13. Liu, C., Sandford, G., Fei, G., and Nicholas, J. (2004) *J. Virol.* **78,** 2460–2471
14. Gruijthuijsen, Y. K., Casarosa, P., Kaptein, S. J. F., Broers, J. L. V., Leurs, R., Bruggeman, C. A., Smit, M. J., and Vink, C. (2002) *J. Virol.* **76,** 1328–1338
15. Verzijl, D., Fitzsimons, C. P., Van Dijk, M., Stewart, J. P., Timmerman, H., Smit, M. J., and Leurs, R. (2004) *J. Virol.* **78,** 3343–3351
16. Okada, T., Sugihara, M., Bondar, A.-N., Elstner, M., Entel, P., and Buss, V. (2004) *J. Mol. Biol.* **342,** 571–583
17. Ballesteros, J. A., and Weinstein, H. (1995) *Methods Neurosci.* **25,** 366–428
18. Jongejan, A., Bruysters, M., J. A., B., Haaksma, E., Bakker, R. A., Pardo, L., and Leurs, R. (2005) *Nat. Chem. Biol.* **1,** 98–103
19. Arvanitakis, L., Geras-Raaka, E., Varma, A., Gershengorn, M. C., and Cesarman, E. (1997) *Nature* **385,** 347–350
20. Rosenkilde, M. M., Kledal, T. N., Brauner-Osborne, H., and Schwartz, T. W. (1999) *J. Biol. Chem.* **274,** 956–961
21. Smit, M. J., Verzijl, D., Casarosa, P., Navis, M., Timmerman, H., and Leurs, R. (2002) *J. Virol.* **76,** 1744–1752
22. Fritze, O., Filipek, S., Kuksa, V., Palczewski, K., Hofmann, K. P., and Ernst, O. P. (2003) *Proc. Natl. Acad. Sci. U. S. A.* **100,** 2290–2295
23. Ho, H. H., Ganeshalingam, N., Rosenhouse-Dantsker, A., Osman, R., and Gershengorn, M. C. (2001) *J. Biol. Chem.* **276,** 1376–1382
24. Palczewski, K., Kumasaka, T., Hori, T., Behnke, C. A., Motoshima, H., Fox, B. A., Trong, I. L., Teller, D. C., Okada, T., Stenkamp, R. E., Yamamoto, M., and Miyano, M. (2000) *Science* **289,** 739–745
25. Lu, Z.-L., Saldanha, J. W., and Hulme, E. C. (2002) *Trends Pharmacol. Sci.* **23,** 140–146
26. Waldhoer, M., Casarosa, P., Rosenkilde, M. M., Smit, M. J., Leurs, R., Whistler, J. L., and Schwartz, T. W. (2003) *J. Biol. Chem.* **278,** 19473–19482
27. Hoare, S., Copland, J. A., Strakova, Z., Ives, K., Jeng, Y.-J., Hellmich, M. R., and Soloff, M. S. (1999) *J. Biol. Chem.* **274,** 28682–28689
28. Kang, D. S., and Leeb-Lundberg, L. M. F. (2002) *Mol. Pharmacol.* **62,** 281–288
29. Sano, T., Ohyama, K., Yamano, Y., Nakagomi, Y., Nakazawa, S., Kikyo, M., Shirai, H., Blank, J. S., Exton, J. H., and Inagami, T. (1997) *J. Biol. Chem.* **272,** 23631–23636
30. Okuno, T., Ago, H., Terawaki, K., Miyano, M., Shimizu, T., and Yokomizo, T. (2003) *J. Biol. Chem.* **278,** 41500–41509

31. Delos Santos, N. M., Gardner, L. A., White, S. W., and Bahouth, S. W. (2006) *J. Biol. Chem.* **281,** 12896–12907
32. Swift, S., Leger, A. J., Talavera, J., Zhang, L., Bohm, A., and Kuliopulos, A. (2006) *J. Biol. Chem.* **281,** 4109–4116
33. Rosenkilde, M. M., McLean, K. A., Holst, P. J., and Schwartz, T. W. (2004) *J. Biol. Chem.* **279,** 32524–32533
34. Bond, R. A., Leff, P., Johnson, T. D., Milano, C. A., Rockman, H. A., McMinn, T. R., Apparsundaram, S., Hyek, M. F., Kenakin, T. P., Allen, L. F., and Lefkowitz, R. J. (1995) *Nature* **374,** 272–276
35. Prioleau, C., Visiers, I., Ebersole, B. J., Weinstein, H., and Sealfon, S. C. (2002) *J. Biol. Chem.* **277,** 36577–36584
36. Natochin, M., Gasimov, K. G., Moussaif, M., and Artemyev, N. O. (2003) *J. Biol. Chem.* **278,** 37574–37581
37. Mirzadegan, T., Benko, G., Filipek, S., and Palczewski, K. (2003) *Biochemistry* **42,** 2759–2767
38. Deupi, X., Olivella, M., Govaerts, C., Ballesteros, J. A., Campillo, M., and Pardo, L. (2004) *Biophys. J.* **86,** 105–115
39. Fan, G.-H., Yang, W., Sai, J., and Richmond, A. (2001) *J. Biol. Chem.* **276,** 16960–16968
40. Fan, G.-H., Yang, W., Wang, X.-J., Qian, Q., and Richmond, A. (2001) *Biochemistry* **40,** 791–800
41. Fan, G.-H., Yang, W., Sai, J., and Richmond, A. (2002) *J. Biol. Chem.* **277,** 6590–6597
42. Simonin, F., Karcher, P., Boeuf, J. J.-M., Matifas, A., and Kieffer, B. L. (2004) *J. Neurochem.* **89,** 766–775
43. Johnson, M. S., Robertson, D. N., Holland, P. J., Lutz, E. M., and Mitchell, R. (2006) *Cell. Signal.* **18,** 1793–1800
44. Holst, P. J., Rosenkilde, M. M., Manfra, D., Chen, S.-C., Wiekowski, M. T., Holst, B., Cifire, F., Lipp, M., Schwartz, T. W., and Lira, S. A. (2001) *J. Clin. Investig.* **108,** 1789–1796